Design and Application of Quadratic Correlation Filters for Target Detection

ABHIJIT MAHALANOBIS
ROBERT R. MUISE
S. ROBERT STANFILL
Lockheed Martin
ALAN VAN NEVEL
Naval Air Warfare Center

We introduce a method for designing and implementing quadratic correlation filters (QCFs) for shift-invariant target detection in imagery. The QCFs are a quadratic classifier that operates directly on the image data without feature extraction or segmentation. In this sense, the QCFs retain the main advantages of conventional linear correlation filters while offering significant improvements in other respects. Not only is more processing required to detect peaks in the outputs of multiple linear filters, but choosing a winner among them is an error prone task. On the other hand, all channels in a QCF work together to optimize the same performance metric and produce a combined output that leads to considerable simplification of the postprocessing scheme. In addition, QCFs also yield better performance than their linear counterparts for comparable throughput requirements.

Two different methods for designing basis functions that optimize the QCF performance criterion are presented. An efficient architecture for implementing QCFs is discussed along with a case study of the proposed approach for detecting targets in LADAR imagery.

Manuscript received November 15, 2002; revised December 20, 2003; released for publication May 14, 2004.

IEEE Log No. T-AES/40/3/835882.

Refereeing of this contribution was handled by J. T. Barnett.

Authors' addresses: A. Mahalanobis, R. R. Muise, S. R. Stanfill, Lockheed Martin, Missiles and Fire Control, MP 450, 5600 Sandlake Road, Orlando, FL 32819; A. Van Nevel, Image and Signal Processing Branch, Sensor and Signals Sciences Division, Research Dept., Naval Air Warfare Center, Weapons Division, China Lake, CA 93555.

I. INTRODUCTION

We investigate here the problem of detecting targets in the presence of clutter. Specifically, we address the problem of detecting a spatially resolved target surrounded by background. Although the technique described here is applicable to any imaging sensor, we present a case study using LADAR data. It should be noted that the goal is not to classify the targets, but to detect them with as small a false-alarm rate as possible. Considerable work has been done in this area over the past three decades. Popular methods for achieving this goal include statistical techniques based on feature classification [1, 2], model-based techniques [3, 4], and neural-networks [5, 6]. Generally speaking, the potential targets are segmented from the background, boundary edges and internal features are measured, and fitted to either statistical or structural models. These methods work well when there is sufficient number of pixels on the targets and the contrast boundaries are well defined. In general however, the performance of most segmentation based methods suffers considerably when the targets exhibit poor contrast relative to the background, or parts of the target are either obscured or in close proximity to clutter objects. In such cases segmentation is a difficult task.

We focus here on target detection techniques based on signal processing methods that do not require segmentation. The leading approach is based on the use of correlation filters [7, 8]. Perhaps the earliest and well known among these is the matched spatial filter (MSF) [9]. Although the MSF is optimum for the detection of a single (deterministic) pattern in the presence of additive white gaussian noise (AWGN), it is hardly suitable for robust detection and recognition of targets in real-world images. For our case however, to add robustness and distortion tolerance to the detection process, we consider the data and the pattern as both being a stochastic process. This no longer fits the model in which the MSF is optimal and a different methodology is needed to define correlators for the detection problem. As a result, many approaches have been proposed for the design of filters for correlators that exhibit robust behavior in the presence of clutter and wide variations in the targets' signatures.

We introduce a new type of quadratic correlation filter (QCF) that improves on linear correlation filters, but retains the advantage of shift-invariance without requiring segmentation or registration. It is well known that the main advantage of linear correlation filters [6–8] is that shift-invariance is inherently obtained, and no explicit segmentation and feature extraction is required. The disadvantage is that a large number of linear filters are required to handle a wide range of variations. Moreover, the filters are usually designed separately, and their outputs are independently processed to select a winner. Searching

multiple output planes is often a time consuming process, and prone to decision errors.

To overcome such limitations of linear correlation filters, we address the target detection objective by formulating it as a quadratic filter design problem. A major benefit of QCFs is the overall reduction in processing complexity and simplification of the decision process. It is shown in Sections II and III that although the QCF requires several linear filters in parallel, these branches work together to implement one quadratic filter, and their outputs are combined into a single detection surface. This greatly simplifies postprocessing complexity as the need to search many separate correlation surfaces is eliminated. Before reviewing the literature on correlation filters further, we first compare and contrast linear discriminat functions (LDFs) [10] and correlation filters both of which are linear filters. Towards this end, consider a linear filter $h(n)$ and an input signal $x(n)$, both of length N. The filter's response to the input signal is given by the usual correlation equation

$$g(n) = \sum_{k=1}^{N} h(k)x(k+n). \tag{1}$$

Each sample of the sequence $g(n)$ is the output of the filter corresponding to a shifted position of the input signal. It is however common in literature to refer to the value $y = g(0)$ as the output of the filter (i.e., corresponding to the case when the filter and the signal are fully overlapped). Let $\mathbf{h} = [h(0)\ \ h(1)\cdots h(N-1)]^{\mathrm{T}}$ be a column vector whose elements are the samples of the filter $h(n)$ of length N, and $\mathbf{x} = [x(0)\ \ x(1)\cdots x(N-1)]^{\mathrm{T}}$ be a vector that represents the input signal $x(n)$. Then, the "output" of a linear filter is given by

$$y = \mathbf{h}^{\mathrm{T}}\mathbf{x} = g(0) = \sum_{k=1}^{N} h(k)x(k). \tag{2}$$

Much work has been done on the design of the filter vector $\mathbf{h}$ so that the output y can be used for pattern recognition [10]. Conventional LDFs seek a solution for $\mathbf{h}$ without any consideration for the full cross-correlation expression in (1). Typically, it is assumed that $\mathbf{x}$ represents a feature vector, and registration of the signal and the filter is not an issue.

When $x(n)$ is a temporal or spatial signal (and not a feature vector), it is generally not known a priori where in the input stream the signal of interest will occur. In this case the filter must search the entire input signal, and produce a maximum response (temporal or spatial) at the location of the best match. In addition to separating the classes, the design of $\mathbf{h}$ must now suppress the responses at false locations of the target, and minimize the impact of background clutter. Linear filters designed with such constraints (taking the full correlation in (1) into account) are referred to as correlation filters, and may be viewed as a superset of conventional LDFs that only give attention to quantity in (2). Considerations that are germane to the design of correlation filters are not part of the design of conventional LDFs. As a result the Fisher discriminant function [10] and other LDFs do not perform well in the context of performing the operation in (1) (i.e., for detecting signals of interest at unknown locations), although their ability to separate feature vectors that are preregistered with the filter vector is considerable.

QCFs may be viewed as generalizations of quadratic discriminant functions that are specialized for detecting targets in images. One of the methods proposed here for the design of QCFs uses the well-known Fukunaga Koontz transform (FKT) [11]. Leger and Lee have shown that general linear transformation of images can be implemented using correlation [12]. In [13], they used this fact to implement the FKT using a correlator as a linear feature extractor, and discussed the classification of images using two features on a limited set of images. Our work extends these concepts to design and implement a quadratic filter that optimizes a different metric for target detection. The objective in [13] was classification of targets that are assumed to be present in a relatively small image. The detection problem is characterized by searching for potential targets at unknown locations in large images with a low false alarm rate. The distance classifier correlation filters (DCCFs) [14] are another type of QCF that are also designed to address the classification problem, but not detection. Polynomial correlation filters (PCFs) [15] have also been proposed for simultaneously processing several nonlinearly modified versions of the input and in effect constitute nonlinear filters. However, the performance metric of the PCF differs from that proposed for the design of QCFs and its output is a linear function of the filter weights.

The rest of the paper is organized as follows. Section II discusses the formulation of QCFs to address the target detection problem, and a method for designing them using the FKT is presented. Section III outlines an efficient architecture for implementing the quadratic filter using a bank of correlation operations. We also comment on some interesting properties of the quadratic filter based on the FKT in this section. Section IV describes an application of the proposed filter for finding targets in LADAR imagery. Finally Section V summarizes the conclusions of this work, and outlines directions for future work.

II. QUADRATIC CORRELATION FILTERS

In this section, we formulate the target detection problem using QCFs. As stated in Section I, linear correlation filters have been successfully used for addressing the target detection problem. It is however

often necessary to use a large number of linear filters for dealing with challenging detection problems [16]. The disadvantage is that each linear filter is designed to operate independently of the others. As a result the correlation surface of all filters must be individually searched and a winner must be selected. A major benefit of QCFs may be to reduce the processing complexity by requiring fewer overall computations and simplify the decision process. It is shown in Section III that although the QCF requires several parallel linear correlations to implement it, the linear branches work together to implement one QCF, and their outputs are combined into a single detection surface. This greatly simplifies postprocessing complexity as the need to search many separate correlation surfaces is eliminated. Another advantage of quadratic filters is that they are able to better exploit the second order statistics of the data. It is well known that quadratic classifiers are optimum for Gaussian distributions. However, even when the data is not necessarily Gaussian we expect QCFs to perform better than their linear counterparts under general conditions.[1]

The issue of finding targets in background clutter is a two-class pattern recognition problem. Consider an input signal $\mathbf{x} = [x(0)\ \ x(1)\cdots x(N-1)]^{\mathrm{T}}$ that can be either a target (class ω_1) or background (class ω_2). For now we assume that $\mathbf{x}$ is a purely real signal. The output of the quadratic filter is defined as

$$y = \mathbf{x}^{\mathrm{T}}\mathbf{T}\mathbf{x} = \sum_{i=1}^{N}\sum_{j=1}^{N} t_{ij}x(i)x(j). \tag{3}$$

The coefficient matrix $\mathbf{T} = \{t_{ij}\}$ is square and real but otherwise unrestricted. It should be noted that since $\mathbf{T}$ is not restricted to be positive definite, the output y can be either positive or negative. The idea is to determine $\mathbf{T}$ such that y is positive and as large as possible when $\mathbf{x} \in \omega_1$, and negative or as small as possible when $\mathbf{x} \in \omega_2$.

Two methods for determining the coefficient matrix $\mathbf{T} = \{t_{ij}\}$ of the quadratic filter are discussed in this work. The first method in Section IIA is an application of the FKT. The second approach outlined in Section IIB exploits the optimization of a Rayleigh quotient type criterion. How both solutions fit in the efficient signal processing architecture of the quadratic filter is discussed in Section III.

A. Design of Quadratic Filters using the Fukunga Koontz Transform

The FKT has been widely used for separating and clustering in feature spaces [11]. The FKT is a powerful method for separating two classes and operates by mapping the data of two classes into a new space where both classes share the same eigenvectors. In this new space, the basis functions that best represent one class have the least information about the second class. The idea is to use this property of the FKT to determine the coefficient matrix $\mathbf{T}$ such that the objectives of the quadratic filter are achieved. We first review the FKT and then discuss the construction of the coefficient matrix $\mathbf{T}$.

1) *Review of the FKT*: Let $\mathbf{x}$ and $\mathbf{y}$ represent sample vectors from the two different classes ω_1 and ω_2, respectively. For simplicity, we assume that the data is purely real (the theory may be easily generalized to complex data and more than two classes). Although the original FKT is based on the covariance matrix, we use the correlation matrices of the classes in our analysis. Assume that the correlation matrices of the two classes are given by $\Sigma_x = E\{\mathbf{x}\mathbf{x}^{\mathrm{T}}\}$ and $\Sigma_y = E\{\mathbf{y}\mathbf{y}^{\mathrm{T}}\}$, respectively. Here, the superscript $^{\mathrm{T}}$ denotes the transpose operation. Since the data is real, the correlation matrices are positive definite, and their sum can be factorized into the form

$$(\Sigma_x + \Sigma_y) = \Phi\Delta\Phi^{\mathrm{T}} \tag{4}$$

where Φ is a matrix with the eigenvectors of $\Sigma_x + \Sigma_y$ as its columns, and Δ is a diagonal matrix with the corresponding eigenvalues as elements of its main diagonal. Let us define a transform matrix $\mathbf{P} = \Phi\Delta^{-1/2}$. Given that Φ is a unitary transformation, it is easy to show from (4) that

$$\mathbf{P}^{\mathrm{T}}(\Sigma_x + \Sigma_y)\mathbf{P} = \mathbf{I} \qquad \text{or} \qquad \mathbf{P}^{\mathrm{T}}\Sigma_x\mathbf{P} + \mathbf{P}^{\mathrm{T}}\Sigma_y\mathbf{P} = \mathbf{I} \tag{5}$$

where $\mathbf{I}$ is the identity matrix. Hence $\mathbf{P}$ diagonalizes the sum of the two correlation matrices. Let us now consider the effect of transforming the data of both classes by $\mathbf{P}$. Under the transformation, the data can be expressed as $\hat{\mathbf{x}} = \mathbf{P}^{\mathrm{T}}\mathbf{x}$ and $\hat{\mathbf{y}} = \mathbf{P}^{\mathrm{T}}\mathbf{y}$, respectively, and the corresponding correlation matrices of the two classes are

$$\begin{aligned}\mathbf{A} &= E\{\hat{\mathbf{x}}\hat{\mathbf{x}}^{\mathrm{T}}\} = \mathbf{P}^{\mathrm{T}}E\{\mathbf{x}\mathbf{x}^{\mathrm{T}}\}\mathbf{P} = \mathbf{P}^{\mathrm{T}}\Sigma_x\mathbf{P}\\ \mathbf{B} &= E\{\hat{\mathbf{y}}\hat{\mathbf{y}}^{\mathrm{T}}\} = \mathbf{P}^{\mathrm{T}}E\{\mathbf{y}\mathbf{y}^{\mathrm{T}}\}\mathbf{P} = \mathbf{P}^{\mathrm{T}}\Sigma_y\mathbf{P}.\end{aligned} \tag{6}$$

Given (5) however, we easily deduce that

$$\mathbf{A} + \mathbf{B} = \mathbf{I} \Rightarrow \mathbf{A} = \mathbf{I} - \mathbf{B}. \tag{7}$$

In other words, the sum of the transformed correlation matrices of the two classes is equal to the identity matrix. Assume that θ_i is an eigenvector of $\mathbf{A}$ with corresponding eigenvalue λ_i, i.e. $\mathbf{A}\theta_i = \lambda_i\theta_i$. Substituting for $\mathbf{A}$ (using the relation in (7)), we obtain

$$(\mathbf{I} - \mathbf{B})\theta_i = \lambda_i\theta_i \Rightarrow \mathbf{B}\theta_i = (1 - \lambda_i)\theta_i. \tag{8}$$

[1]The reason is that the filtering process produces a nearly Gaussian output (irrespective of the distribution of the input data) for which the quadratic detector is optimum.

Hence it follows that if θ_i is an eigenvector of $\mathbf{A}$, then θ_i is also an eigenvector of $\mathbf{B}$ but corresponding to an eigenvalue of $1-\lambda_i$. Thus in the transformed domain the two classes share the same eigenvectors with complimentary eigenvalues.

A direct consequence of this property of the eigenvalues is that the eigenvector that contains the maximum information about $\hat{\mathbf{x}}$ has the least information about $\hat{\mathbf{y}}$, and vice-versa. It should be further noted that since none of the eigenvalues can be negative, the value of λ_i must range between 0.0 and 1.0.

2) *Construction of the Coefficient Matrix*: We now discuss how to design the coefficient matrix $\mathbf{T}$ in (3) using the basis functions of the FKT. Let $[\theta_1 \ \theta_2 \cdots \theta_N]$ be the N basis function of the FKT that represents the data corresponding to the ordered eigenvalues $\lambda_1 \le \lambda_2 \le \lambda_3 \cdots \le \lambda_N$ of class ω_1. These basis functions are shared by both classes. However, if θ_N is the dominant eigenvector of $\mathbf{A}$, then it is also the weakest eigenvector of $\mathbf{B}$ corresponding to an eigenvalue of $1-\lambda_N$. We use this fact to choose the first N_1 eigenvectors $[\theta_1 \ \theta_2 \cdots \theta_{N_1}]$ that best represent the clutter class ω_2 (i.e., the N_1 strongest eigenvectors of $\mathbf{B}$) and the last N_2 eigenvectors $[\theta_{N-N_2+1} \ \theta_{N-N_2+2} \cdots \theta_N]$ that best represent the target class ω_1. It should be noted that $N_1 + N_2 < N$. Ideally, clutter basis functions are chosen such that $\lambda_i \le \varepsilon$, $1 \le i \le N_1$ while the target basis functions are chosen such that $\lambda_i \ge 1-\varepsilon$, $N-N_2+1 \le i \le N$, and the tolerance ε is an arbitrarily small number.

We then construct the matrices

$$\Theta_y = [\theta_1 \quad \theta_2 \cdots \theta_{N_1}], \qquad \Theta_x = [\theta_{N-N_2+1} \quad \theta_{N-N_2+2} \cdots \theta_N] \tag{9}$$

using the selected basis functions as the columns. Now consider a test vector $\mathbf{z}$ and its transformed version $\hat{\mathbf{z}} = \mathbf{P}^{\mathrm{T}}\mathbf{z}$. The projection of $\hat{\mathbf{z}}$ on these matrices is given by

$$\mathbf{v}_y = \Theta_y^{\mathrm{T}}\hat{\mathbf{z}}, \qquad \mathbf{v}_x = \Theta_x^{\mathrm{T}}\hat{\mathbf{z}}. \tag{10}$$

When $\hat{\mathbf{z}}$ belongs to class ω_1, we expect the value of the elements of $\mathbf{v}_y$ to be generally small in magnitude, whereas the elements of $\mathbf{v}_x$ will tend to be large in magnitude. Similarly, if $\hat{\mathbf{z}}$ belongs to class ω_2, the value of the elements of $\mathbf{v}_x$ will be generally small in magnitude while the elements of $\mathbf{v}_y$ will exhibit large magnitudes. Consider therefore a statistic

$$\begin{aligned}\varphi &= \mathbf{v}_x^{\mathrm{T}}\mathbf{v}_x - \mathbf{v}_y^{\mathrm{T}}\mathbf{v}_y = (\hat{\mathbf{z}}^{\mathrm{T}}\Theta_x\Theta_x^{\mathrm{T}}\hat{\mathbf{z}}) - (\hat{\mathbf{z}}^{\mathrm{T}}\Theta_y\Theta_y^{\mathrm{T}}\hat{\mathbf{z}}) \\ &= \hat{\mathbf{z}}^{\mathrm{T}}(\Theta_x\Theta_x^{\mathrm{T}} - \Theta_y\Theta_y^{\mathrm{T}})\hat{\mathbf{z}}. \end{aligned} \tag{11}$$

It is expected that φ will be positive and large for samples of class ω_1 and small or negative for samples of class ω_2. In fact, it is easy to show that

$$E_1\{\varphi\} = \sum_{i=N-N_2+1}^{N} \lambda_i - \sum_{i=1}^{N_1} \lambda_i \tag{12}$$

where $E_i\{\cdot\}$ indicates the expectation operation performed over class ω_i. A lower bound on $E_1\{\varphi\}$ in terms of the tolerance ε and the number of basis functions chosen can be obtained as follows. We note that the largest eigenvalues satisfy $\lambda_i \ge 1-\varepsilon$, whereas the smallest eigenvalues satisfy $\lambda_i \le \varepsilon$. This yields

$$\begin{aligned} E_1\{\varphi\} &\ge N_2(1-\varepsilon) - N_1\varepsilon \\ &\ge N_2 - (N_2+N_1)\varepsilon. \end{aligned} \tag{13}$$

Similary, the expected value of the statistic over the class ω_2 is

$$\begin{aligned} E_2\{\varphi\} &= \sum_{i=N-N_2+1}^{N} (1-\lambda_i) - \sum_{i=1}^{N_1} (1-\lambda_i) \\ &= N_2 - N_1 - \left(\sum_{i=N-N_2+1}^{N} \lambda_i - \sum_{i=1}^{N_1} \lambda_i \right) \\ &= N_2 - N_1 - E_1\{\varphi\}. \end{aligned} \tag{14}$$

Consequently $E_2(\varphi)$ decreases as $E_1(\varphi)$ increases, and is forced to be either small or negative. An upper bound on $E_2(\varphi)$ is given by

$$\begin{aligned} E_2\{\varphi\} &\le N_2 - N_1 - (N_2 - (N_2+N_1)\varepsilon) \\ &\le (N_2+N_1)\varepsilon - N_1. \end{aligned} \tag{15}$$

Finally, the separation between the expected value of φ for the two classes is

$$E_1\{\varphi\} - E_2\{\varphi\} = \sum_{i=N-N_2+1}^{N} (2\lambda_i - 1) - \sum_{i=1}^{N_1} (2\lambda_i - 1). \tag{16}$$

Using the expression for the bounds on $E_1(\varphi)$ and $E_2(\varphi)$, it follows that

$$E_1\{\varphi\} - E_2\{\varphi\} \ge (N_1+N_2)(1-2\varepsilon). \tag{17}$$

The quantity in (16) reflects the separability between the two classes achieved using the statistic in (11). The expression in (17) indicates that this is made as large as possible by choosing those eigenvalues for which ε is as small as possible. Specific guidelines for choosing the number of basis functions that lead to the maximum separation is discussed further by means of an example in Section IV.

The statistic φ in (11) is expressed in terms of the transformed data $\hat{\mathbf{z}}$. Substituting $\hat{\mathbf{z}} = \mathbf{P}^{\mathrm{T}}\mathbf{z}$, we obtain

$$\varphi = \mathbf{z}^{\mathrm{T}}\mathbf{P}(\Theta_x\Theta_x^{\mathrm{T}} - \Theta_y\Theta_y^{\mathrm{T}})\mathbf{P}^{\mathrm{T}}\mathbf{z} = \mathbf{z}^{\mathrm{T}}\mathbf{T}\mathbf{z} \tag{18}$$

where

$$\mathbf{T} = \mathbf{P}(\Theta_x\Theta_x^{\mathrm{T}} - \Theta_y\Theta_y^{\mathrm{T}})\mathbf{P}^{\mathrm{T}} \tag{19}$$

is the desired coefficient matrix of the quadratic filter defined in (3). It should be noted that $\mathbf{T}$ is a symmetric square matrix but neither full rank nor positive definite.

B. Alternate Methods for Designing the Coefficient Matrix

While the FKT is only one approach to the design of the coefficient matrix for QCFs, other approaches are also possible. To demonstrate this, we present a QCF design approach that optimizes the separation metric $E_1\{\varphi\} - E_2\{\varphi\}$ by formulating the problem as a Rayleigh quotient. The generalized Rayleigh quotient of the vector $\mathbf{x}$ is defined as

$$J(\mathbf{x}) = \frac{\mathbf{x}^{\mathrm{T}}\mathbf{A}\mathbf{x}}{\mathbf{x}^{\mathrm{T}}\mathbf{B}\mathbf{x}} \tag{20}$$

where $\mathbf{B}$ is invertible. It can be shown that $J(\mathbf{x})$ is maximized by selecting $\mathbf{x}$ to be the dominant eigenvector of $\mathbf{B}^{-1}\mathbf{A}$, and that the maximum value of Rayleigh quotient is equal to its largest eigenvalue.

A similar method has been used earlier by Mahalanobis and Singh [17] to design linear filters that can be used to separate textures. Let us assume that the $d \times d$ coefficient matrix $\mathbf{T}$ is defined as

$$\mathbf{T} = \mathbf{T}_A - \mathbf{T}_B \tag{21}$$

where

$$\mathbf{T}_A = \sum_{i=1}^{N_1} \gamma_i \mathbf{q}_i \mathbf{q}_i^{\mathrm{T}}, \qquad \mathbf{T}_B = \sum_{i=1}^{N_2} \delta_i \mathbf{p}_i \mathbf{p}_i^{\mathrm{T}} \tag{22}$$

and $\mathbf{q}_i$, $1 \le i \le N_1$, and $\mathbf{p}_i$, $1 \le i \le N_2$ are a set of orthonormal vectors. Furthermore, let $\mathbf{x}$ be a sample vector to be classified as either class ω_1 or ω_2 based on the statistic $\varphi(\mathbf{x}) = \mathbf{x}^{\mathrm{T}}\mathbf{T}\mathbf{x}$. It is desired that $\varphi(\mathbf{x})$ should be positive and as large as possible if $\mathbf{x} \in \omega_1$, and conversely $\varphi(\mathbf{x})$ should be as small as possible or negative if $\mathbf{x} \in \omega_2$. To achieve this, we seek the coefficient matrix that maximizes the function

$$\begin{aligned} E_1\{\varphi\} - E_2\{\varphi\} &= E_1\{\mathbf{x}^{\mathrm{T}}\mathbf{T}\mathbf{x}\} - E_2\{\mathbf{x}^{\mathrm{T}}\mathbf{T}\mathbf{x}\} \\ &= E_1\{\mathbf{x}^{\mathrm{T}}(\mathbf{T}_A - \mathbf{T}_B)\mathbf{x}\} - E_2\{\mathbf{x}^{\mathrm{T}}(\mathbf{T}_A - \mathbf{T}_B)\mathbf{x}\} \\ &= E_1\{\mathbf{x}^{\mathrm{T}}\mathbf{T}_A\mathbf{x}\} - E_2\{\mathbf{x}^{\mathrm{T}}\mathbf{T}_A\mathbf{x}\} \\ &\quad + E_2\{\mathbf{x}^{\mathrm{T}}\mathbf{T}_B\mathbf{x}\} - E_1\{\mathbf{x}^{\mathrm{T}}\mathbf{T}_B\mathbf{x}\} \\ &= J_A + J_B \end{aligned} \tag{23}$$

where $E_i\{\cdot\}$ indicates the expectation operation performed over class ω_i, and

$$\begin{aligned} J_A &= E_1\{\mathbf{x}^{\mathrm{T}}\mathbf{T}_A\mathbf{x}\} - E_2\{\mathbf{x}^{\mathrm{T}}\mathbf{T}_A\mathbf{x}\} \\ J_B &= E_2\{\mathbf{x}^{\mathrm{T}}\mathbf{T}_B\mathbf{x}\} - E_1\{\mathbf{x}^{\mathrm{T}}\mathbf{T}_B\mathbf{x}\}. \end{aligned} \tag{24}$$

Our approach will be to determine $\mathbf{T}_A$ and $\mathbf{T}_B$ separately such that J_A and J_B are each as large as possible. The first term in the expression for J_A in (24) can be written as

$$\begin{aligned} E_1\{\mathbf{x}^{\mathrm{T}}\mathbf{T}_A\mathbf{x}\} &= E_1\left\{\sum_{i=1}^{N_1} \gamma_i \mathbf{x}^{\mathrm{T}}\mathbf{q}_i\mathbf{q}_i^{\mathrm{T}}\mathbf{x}\right\} \\ &= E_1\left\{\sum_{i=1}^{N_1} \gamma_i \mathbf{q}_i^{\mathrm{T}}\mathbf{x}\mathbf{x}^{\mathrm{T}}\mathbf{q}_i\right\} = \sum_{i=1}^{N_1} \gamma_i \mathbf{q}_i^{\mathrm{T}}\mathbf{R}_1\mathbf{q}_i \end{aligned} \tag{25}$$

where $\mathbf{R}_1 = E_1\{\mathbf{x}\mathbf{x}^{\mathrm{T}}\}$ is the correlation matrix of class ω_1. Similarly, the second term of J_A can be expressed as $E_2\{\mathbf{x}^{\mathrm{T}}\mathbf{T}_A\mathbf{x}\} = \sum_{i=1}^{N_1} \gamma_i \mathbf{q}_i^{\mathrm{T}}\mathbf{R}_2\mathbf{q}_i$ where $\mathbf{R}_2 = E_2\{\mathbf{x}\mathbf{x}^{\mathrm{T}}\}$ is the correlation matrix of class ω_2. Therefore J_A can be written as

$$J_A = \sum_{i=1}^{N_1} \gamma_i \mathbf{q}_i^{\mathrm{T}}\mathbf{R}_1\mathbf{q}_i - \sum_{i=1}^{N_1} \gamma_i \mathbf{q}_i^{\mathrm{T}}\mathbf{R}_2\mathbf{q}_i = \sum_{i=1}^{N_1} \gamma_i \mathbf{q}_i^{\mathrm{T}}(\mathbf{R}_1 - \mathbf{R}_2)\mathbf{q}_i. \tag{26}$$

One approach to ensure that J_A is positive and large is to choose $\mathbf{q}_i$ to be the eigenvectors of $\mathbf{R}_1 - \mathbf{R}_2$ that correspond to its positive eigenvalues, and the weights γ_i according to the rule

$$\gamma_i = \begin{cases} 1 & \mathbf{q}_i^{\mathrm{T}}(\mathbf{R}_1 - \mathbf{R}_2)\mathbf{q}_i > 0 \\ 0 & \text{otherwise} \end{cases}. \tag{27}$$

Since $\mathbf{R}_1$ and $\mathbf{R}_2$ are positive definite, the objective of making the terms $\mathbf{q}_i^{\mathrm{T}}(\mathbf{R}_1 - \mathbf{R}_2)\mathbf{q}_i$ in (26) (and hence J_A) positive and large can be also achieved by making the ratio

$$J(\mathbf{q}_i) = \frac{\mathbf{q}_i^{\mathrm{T}}\mathbf{R}_1\mathbf{q}_i}{\mathbf{q}_i^{\mathrm{T}}\mathbf{R}_2\mathbf{q}_i} \tag{28}$$

large. Of course, the dominant eigenvector of $\mathbf{R}_2^{-1}\mathbf{R}_1$ yields the maximum value of the Rayleigh quotient in (28) and is the best choice for the first vector, say $\mathbf{q}_1$. However, under the constraint that $\{\mathbf{q}_i\}$ are linearly independent and unit norm basis vectors, the eigenvectors of $\mathbf{R}_2^{-1}\mathbf{R}_1$ that correspond to eigenvalues greater than unity are good choices for $\mathbf{q}_i$. In this case, the rule for the weights γ_i is therefore

$$\gamma_i = \begin{cases} 1 & \mathbf{q}_i^{\mathrm{T}}(\mathbf{R}_2^{-1}\mathbf{R}_1)\mathbf{q}_i > 1 \\ 0 & \text{otherwise} \end{cases}. \tag{29}$$

Whether $\mathbf{q}_i$ are chosen as the eigenvectors of $\mathbf{R}_1 - \mathbf{R}_2$ or $\mathbf{R}_2^{-1}\mathbf{R}_1$, the resulting matrix $\mathbf{T}_A$ yields a large and positive value of J_A.

We now consider the matrix $\mathbf{T}_B$ and the choice of the vectors $\mathbf{p}_i$. Following a procedure similar to that used for the treatment of J_A, we observe that

$$J_B = \sum_{i=1}^{N_2} \delta_i \mathbf{p}_i^{\mathrm{T}}\mathbf{R}_2\mathbf{p}_i - \sum_{i=1}^{N_2} \delta_i \mathbf{p}_i^{\mathrm{T}}\mathbf{R}_1\mathbf{p}_i = \sum_{i=1}^{N_2} \delta_i \mathbf{p}_i^{\mathrm{T}}(\mathbf{R}_2 - \mathbf{R}_1)\mathbf{p}_i. \tag{30}$$

Hence J_B can be made large and positive by choosing $\mathbf{p}_i$ to be the eigenvectors of $\mathbf{R}_2 - \mathbf{R}_1$ with

weights δ_i chosen according to the rule

$$\delta_i = \begin{cases} 1 & \mathbf{p}_i^{\mathrm{T}}(\mathbf{R}_2 - \mathbf{R}_1)\mathbf{p}_i > 0 \\ 0 & \text{otherwise} \end{cases}. \tag{31}$$

Alternatively, the vectors $\mathbf{p}_i$ may be chosen as the eigenvectors of $\mathbf{R}_1^{-1}\mathbf{R}_2$ with weights δ_i given by

$$\delta_i = \begin{cases} 1 & \mathbf{p}_i^{\mathrm{T}}(\mathbf{R}_1^{-1}\mathbf{R}_2)\mathbf{p}_i > 1 \\ 0 & \text{otherwise} \end{cases}. \tag{32}$$

Whether $\mathbf{p}_i$ are chosen as the eigenvectors of $\mathbf{R}_2 - \mathbf{R}_1$ or $\mathbf{R}_1^{-1}\mathbf{R}_2$, the resulting matrix $\mathbf{T}_B$ yields a large and positive value of J_B.

Numerical optimization techniques may be also used to search for optimum values of weights γ_i and δ_i. Several interesting differences exist between the Rayleigh quotient formulation and the solution based on the FKT. For example, the basis functions obtained via this approach are unit norm whereas those based on the FKT are not and a different weighting scheme for the QCF outputs is realized. The Rayleigh quotient method and other design techniques for QCFs will be further explored in future publications.

III. AN EFFICIENT ARCHITECTURE FOR IMPLEMENTING THE QUADRATIC FILTER

Consider now the problem of processing an entire 2D image using the quadratic filter in (3). Let us assume that the vector $\mathbf{z}$ is obtained by lexicographically reordering the data in a relatively small window of size $r \times c$ within a much larger image of size $R \times C$.[2] The complexity of the direct computation necessary to evaluate the expression in (3) at all overlapping $r \times c$ subregions of the image is rather large. We therefore seek an efficient architecture for obtaining the full correlation of the input scene and the quadratic filter.

Denoting the dimensionality of the space by $d = r \cdot c$, let us assume that the $d \times d$ coefficient matrix $\mathbf{T}$ of rank N can be expressed as $\mathbf{T} = \mathbf{F}\mathbf{F}^{\mathrm{T}}$, where $\mathbf{F} = [\mathbf{f}_1\ \mathbf{f}_2 \cdots \mathbf{f}_N]$ is a $d \times N$ matrix ($N \leq d$). We note that the output of the quadratic filter at a particular location can be expressed as

$$y = \mathbf{z}^{\mathrm{T}}\mathbf{T}\mathbf{z} = \mathbf{z}^{\mathrm{T}}\mathbf{F}\mathbf{F}^{\mathrm{T}}\mathbf{z} = \mathbf{v}^{\mathrm{T}}\mathbf{v} \tag{33}$$

where $\mathbf{v} = [v_1\ v_2 \cdots v_N]^{\mathrm{T}}$ is a vector of the projection of $\mathbf{z}$ on the N columns of $\mathbf{F}$. Clearly, $\mathbf{v}$ is a function of the spatial region of the image that is represented by $\mathbf{z}$. The question is how can the elements of $\mathbf{v}$ be computed over the entire scene using efficient signal processing methods. Let $x(m,n)$ represent the full image to be processed. Furthermore, let us reorder the elements of $\mathbf{f}_i$ into an $r \times c$ mask $f_i(m,n)$. It is then easy to see that the value of v_i (i.e., ith element of $\mathbf{v}$) at all locations within the image can be obtained via the 2D correlation of $f_i(m,n)$ and $x(m,n)$ as

$$v_i(m,n) = x(m,n) \otimes f_i(m,n), \qquad 1 \leq i \leq N \tag{34}$$

where the symbol $\otimes$ indicates the 2D correlation operation. Here, we have expressed v_i along with the indices (m,n) to indicate that it is a function of the location of $\mathbf{z}$ in the image.

The samples of $v_i(m,n)$ can be viewed as a partial result at each point in the image obtained by projecting the $r \times c$ region of the image centered at that point on $\mathbf{f}_i$. To obtain the quadratic term in (33) for all points in the image, it now remains to square the pixels of the partial results and add them. Therefore, the output of the quadratic filter for all points in the image is given by

$$y(m,n) = \sum_{i=1}^{N} |v_i(m,n)|^2 = \sum_{i=1}^{N} |x(m,n) \otimes f_i(m,n)|^2. \tag{35}$$

The expression in (35) is a succint way to express the output of the quadratic filter in response to the full input image. The computations can be readily dealt with using N 2D cross-correlation operation, each of which is efficiently implemented using fast Fourier transforms (FFTs).

Let us now discuss the implementation of the specific solution for $\mathbf{T}$ in (19). By defining $\mathbf{F} = \mathbf{P}\Theta_x$ and $\mathbf{G} = \mathbf{P}\Theta_y$ we can write the coefficient matrix as

$$\mathbf{T} = \mathbf{F}\mathbf{F}^{\mathrm{T}} - \mathbf{G}\mathbf{G}^{\mathrm{T}}. \tag{36}$$

Other than the fact that $\mathbf{T}$ here is a difference of two terms, the solution follows the same form as the general case described in (35). The output of the quadratic filter in response to the full image also involves two terms and takes on the form

$$y(m,n) = \sum_{i=1}^{N_2} |x(m,n) \otimes f_i(m,n)|^2 - \sum_{i=1}^{N_1} |x(m,n) \otimes g_i(m,n)|^2 \tag{37}$$

where $f_i(m,n)$ and $g_i(m,n)$ are the ith columns of $\mathbf{F}$ and $\mathbf{G}$, respectively, each reshaped into an $r \times c$ mask.

Fig. 1 depicts the architecture required to efficiently process a full image with the quadratic filter. Essentially, the input image is correlated with a bank of linear filters to obtain partial results that are squared and added to obtain the desired quadratic output for every point in the input image. Although several branches of linear filters are required, the architecture shown comprises a single quadratic filter. Since each of the branches can be implemented using FFTs, the number of multiplications required in the architecture in Fig. 1 is proportional to $N\log(rc)$ where N is the number of branches, and $r \times c$ is the size of the filter masks. In comparison, the number of multiplications required for the direct computation

[2]Typical sizes of real-world images may be 340×480 pixels (or larger) whereas the window size for $\mathbf{x}$ may be 20×40, chosen to be approximately the size of targets of interest.

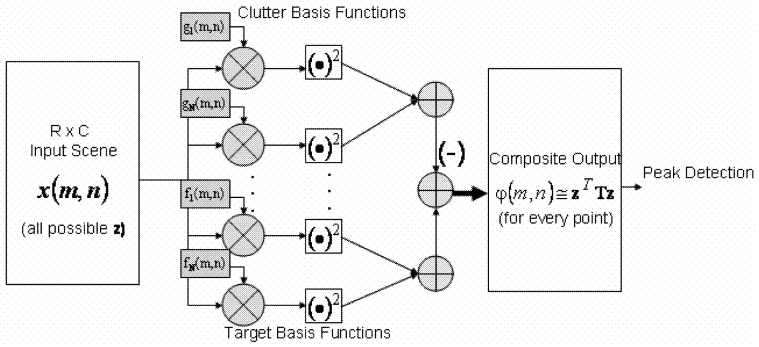

Fig. 1. Efficient architecture for implementing the quadratic filter correlates input image with bank of linear filters to obtain partial results that are squared and added to obtain the desired quadratic output for every point in input image.

of the quadratic term at every point is proportional to $(rc)^2$. For typical numbers such as $N = 30$, $r = 20$, $c = 40$, this can imply a speed up by a factor of over 2000 compared with the brute-force computation of the statistic over the whole image.

The architecture of the QCF in Fig. 1 is general in that any set of basis functions can be implemented. We refer to the set of basis functions that optimize the statistic of interest in the context of the quadratic filter architecture in Fig. 1 as tuned basis functions (TBFs). While the FKT represents one method for designing TBFs for quadratic filters, we note that other approaches (such as a Rayleigh quotient formulation of the performance metric) are also feasible, and that they can be all implemented via the architecture in Fig. 1.

A. Some Subtleties and Properties of the TBFs

As a correlation filter, the TBFs must be able to detect targets by producing a strong response at their true location or desired aimpoint. In other words, not only is it necessary to reject clutter, but it is also important to reject false (off-set) positions of the targets. To achieve this, the original linear correlation filters (such as the MACE filter [7]) minimized a quadratic term proportional to the energy in the correlation surface while constraining the response to the target.[3] In the case of the TBFs, this subtle point factors in to the definition of Σ_y, the correlation matrix of the class to be rejected.

Specifically we define $\Sigma_y = \Sigma_C + \Sigma_D$ to be comprised of two components: the clutter correlation matrix Σ_C, and Σ_D, the correlation matrix that represents shifted versions of the targets that are off-set from their true center. Including Σ_D in the definition of Σ_y enables the TBF to produce a narrower response to the target (that is closer to the correct aimpoint) by inhibiting its response to off-set positions of the target. This is also desirable for the clutter or noise class since all shifted versions of the clutter images must be also rejected. It is easy to show that the correlation matrices become Toeplitz if all shifted versions of the training images are used in the estimation. Thus both Σ_C and Σ_D, and hence Σ_y are Toeplitz.

An interesting property of the TBFs is that the elements of $\mathbf{v}$ are decorrelated. To prove this it is easy to show that the matrix $E\{\mathbf{v}\mathbf{v}^{\mathrm{T}}\}$ is diagonal. Using the definitions in (10) we see that if

$$\mathbf{v} = [\mathbf{v}_y \quad \mathbf{v}_x] = [\Theta_y \quad \Theta_x]^{\mathrm{T}}\hat{\mathbf{z}}, \qquad \text{then}$$
$$E_1\{\mathbf{v}\mathbf{v}^{\mathrm{T}}\} = E_1\{[\Theta_y \quad \Theta_x]^{\mathrm{T}}\hat{\mathbf{z}}\hat{\mathbf{z}}^{\mathrm{T}}[\Theta_y \quad \Theta_x]\}. \tag{38}$$

Noting that $E_1\{\hat{\mathbf{z}}\hat{\mathbf{z}}^{\mathrm{T}}\} = \mathbf{A}$ is the correlation matrix of class ω_1 in the domain of the FKT, it is easy to see that

$$E_1\{\mathbf{v}\mathbf{v}^{\mathrm{T}}\} = \begin{bmatrix} \Theta_y^{\mathrm{T}}\mathbf{A}\Theta_y & \Theta_x^{\mathrm{T}}\mathbf{A}\Theta_y \\ \Theta_y^{\mathrm{T}}\mathbf{A}\Theta_x & \Theta_x^{\mathrm{T}}\mathbf{A}\Theta_x \end{bmatrix}. \tag{39}$$

Since the columns of Θ_y and Θ_x are the eigenvectors of $\mathbf{A}$, it is follows that

$$E_1\{\mathbf{v}\mathbf{v}^{\mathrm{T}}\} = \begin{bmatrix} \lambda_1 & & & & & \\ & \ddots & & 0 & & \\ & & \lambda_{N_1} & & & \\ & & & \lambda_{N-N_2+1} & & \\ & 0 & & & \ddots & \\ & & & & & \lambda_N \end{bmatrix}. \tag{40}$$

Owing to the central limit theorem and some mixing or decorrelation in original variables, it is likely that the elements of $\mathbf{v}$ will behave like Gaussian random variables. Therefore, the elements of $\mathbf{v}$ can be treated as independent random variables. For the Gaussian case it is well known that a quadratic classifier is optimum, and therefore the QCF proposed here is expected to perform well.

[3]The MACE filter is of the form $\mathbf{h} = \mathbf{D}^{-1}\mathbf{X}(\mathbf{X}^{+}\mathbf{D}^{-1}\mathbf{X})^{-1}\mathbf{u}$, where $\mathbf{D}$ represents the power spectrum of the data vectors in $\mathbf{X}$. The filter $\mathbf{h}$ minimizes the correlation energy $\mathbf{h}^{+}\mathbf{D}\mathbf{h}$ while yielding the desired output $\mathbf{X}^{+}\mathbf{h} = \mathbf{u}$ in response to the data.

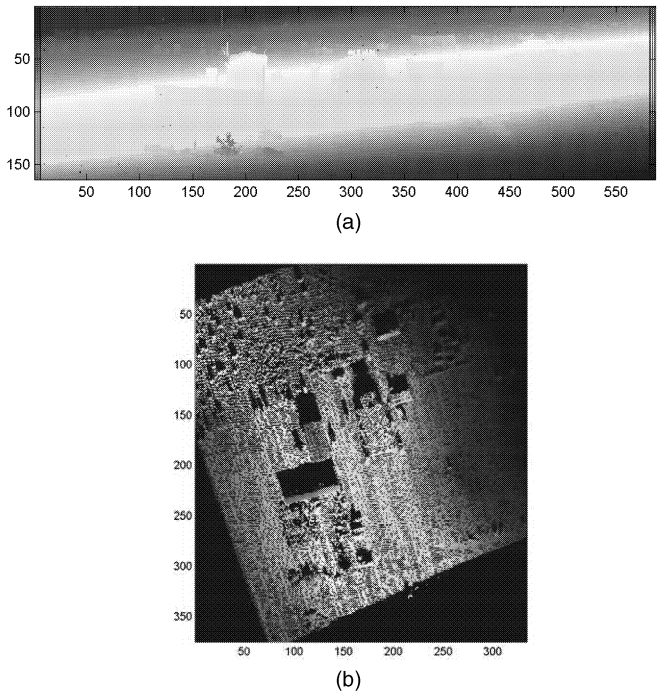

Fig. 2. LADAR data (a) is measurement of range from sensor to each point in the scene. Nadir view (b) can be obtained by projecting data on to rectified grid. Shadows appear in regions where data was not available.

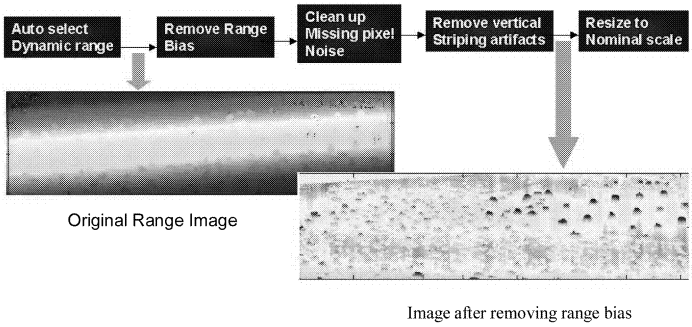

Fig. 3. Target information in LADAR imagery is enhanced by removing various artifacts and range bias.

It is interesting to note that $\mathbf{F}$ and $\mathbf{G}$ (of (36)) are not an orthonormal basis set. Since $\mathbf{F} = \mathbf{P}\Theta_x$, and $\mathbf{G} = \mathbf{P}\Theta_y$ we observe that

$$\begin{aligned}\mathbf{F}^{\mathrm{T}}\mathbf{F} &= \Theta_x^{\mathrm{T}}\mathbf{P}^{\mathrm{T}}\mathbf{P}\Theta_x = \Theta_x^{\mathrm{T}}\Delta^{-1}\Theta_x \\ \mathbf{G}^{\mathrm{T}}\mathbf{G} &= \Theta_y^{\mathrm{T}}\mathbf{P}^{\mathrm{T}}\mathbf{P}\Theta_y = \Theta_y^{\mathrm{T}}\Delta^{-1}\Theta_y\end{aligned} \tag{41}$$

are not the identity matrix. In fact, the norm of the columns of $\mathbf{F}$ and $\mathbf{G}$ are weighted inversely by the eigenvalues of the matrix $(\Sigma_x + \Sigma_y)$. This attenuates the dominant basis functions while the weaker ones are emphasized. In practice, this helps to represent the weaker characteristics of the data on an equal basis with the strongest information.

IV. EXAMPLE OF TARGET DETECTION IN LADAR IMAGERY

In this section, we describe the performance of TBFs designed to detect a target in LADAR imagery. An example of LADAR range imagery is shown in Fig. 2(a). The pixel values represent range measurements from the sensor to every point in the scene. In fact, the data can be manipulated to create such views from any arbitrary direction. Of course, some regions of the scene may not be visible where data is not available due to either shadows or obstructions. Examples of LADAR range image from different angles is shown in Fig. 2.

To facilitate detection of targets in range imagery, it is first necessary to remove the range bias introduced by the measurement process. In other words, what is often of interest is not the distance of the object from the sensor, but the modulation in the range measurement induced by the shape and size of the object. To enhance this information, we estimate the range to the ground plane at every point, and subtract it from the image. This is illustrated in Fig. 3 where the targets are in the raw range image on the left in are difficult to visualize. The image on the right in Fig. 3 is the result of removing the estimated

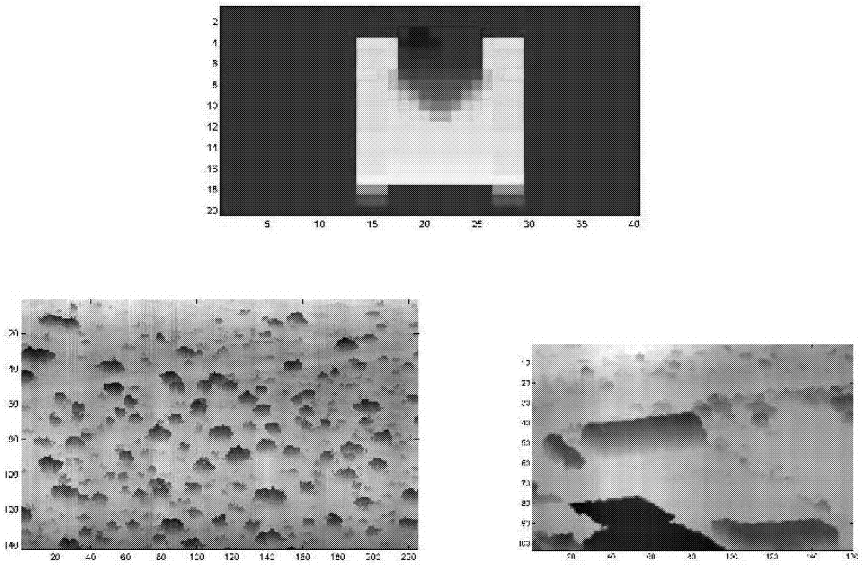

Fig. 4. Sample images of synthetic target image (top) and clutter (bottom). Both natural and man-made clutter shown.

ground plane (range bias) and the targets are now visually prominent.

The target rich area shown in Fig. 3 was used to assess the performance of the TBFs for detecting the M60 tanks in particular. There are several M60s in the scene, some of which are in the clear and others are partially obscured. The data from several passes over this site was used to analyze the performance of the algorithm. In each pass, all frames between the ranges of 700 m–1200 m were included in the test. In all, there were over 1000 possible target detection opportunities. No penalty was assessed if a non-M60 target was detected (as discrimination is not a goal for the detector), but it was also not counted as a part of the detection list.

A software tool was available to generate synthetic views of the target. The TBFs were synthesized using synthetic images of an M60 target, and natural and man-made clutter shown in Fig. 4. The target data was generated every 2° in azimuth to cover all aspects, and between the elevations of 15° and 30° in increments of 3°. The images were of size 20×40, and generated at a range of 1200 m. Since the range bias is removed, the background was set to zero. The resulting eigenvalues of the two classes and examples of the best target and clutter TBFs are shown in Fig. 5.

Although the dimensionality of the space is 800, it was necessary to retain only 200 basis functions in the definition of **P** due to the compaction property of the Karhunen-Loève transform [18] (i.e., **P** is a 800×200 matrix). Let us now consider the plots of the eigenvalues of the FKT shown in Fig. 5. These plots reflect the results of transforming a set of 20×40 images of two classes by the matrix **P** as described in Section IIA, and computing the eigenvectors and eigenvalues of the correlation matrices in the transformed space. In Fig. 5, the horizontal axis is the eigenvalue number. Of course by construction, both classes have the same eigenvectors. The red curve shows the eigenvalues of the clutter class whereas the blue curve reflects the eigenvalues of the target class. It is easily seen that the two curves are complements of each other. For instance, we see that eigenvector number 200 has an eigenvalue of $\lambda = 0.9$ associated with the target class (blue curve), while the clutter eigenvalue for the same eigenvector is $1 - \lambda = 0.1$ (red curve). Another way to interpret this is to say that eigenvector number 200 contains 90% information about the target and only 10% information about the clutter. In fact, the TBF based on this eigenvector is shown in the top left corner of Fig. 5. Similarly, the first eigenvector has only information about clutter (100%) (none about the target), and is shown in the top right corner of the figure.

The two curves in Fig. 5 cross over at eigenvector number 182. This particular eigenvector therefore has equal amount of information about both clutter and target (eigenvalue is 0.5 for both classes). It may be said that all eigenvectors to the right of the cross over point (183 and higher) are better for representing target whereas those to the left (between 1 and 182) are better for characterizing clutter. A plot of the separation metric of (16) is shown in Fig. 6. This plot was obtained by assuming that $N_1 + N_2 = N = 200$ (i.e., if the first N_1 basis functions are used for representing clutter then the remaining N_2 basis functions are used for representing target). Not surprisingly, we see that $E_1\{\varphi\} - E_2\{\varphi\}$ is maximum when $N_1 = 182$, and $N_2 = 18$. Thus, the best performance for acquiring the targets with the smallest false alarm rate should be achieved using the last 18 of the 200 TBFs as the functions $f_i(m,n)$ in (37), and the first 182 TBFs as $g_i(m,n)$ in the same equation.

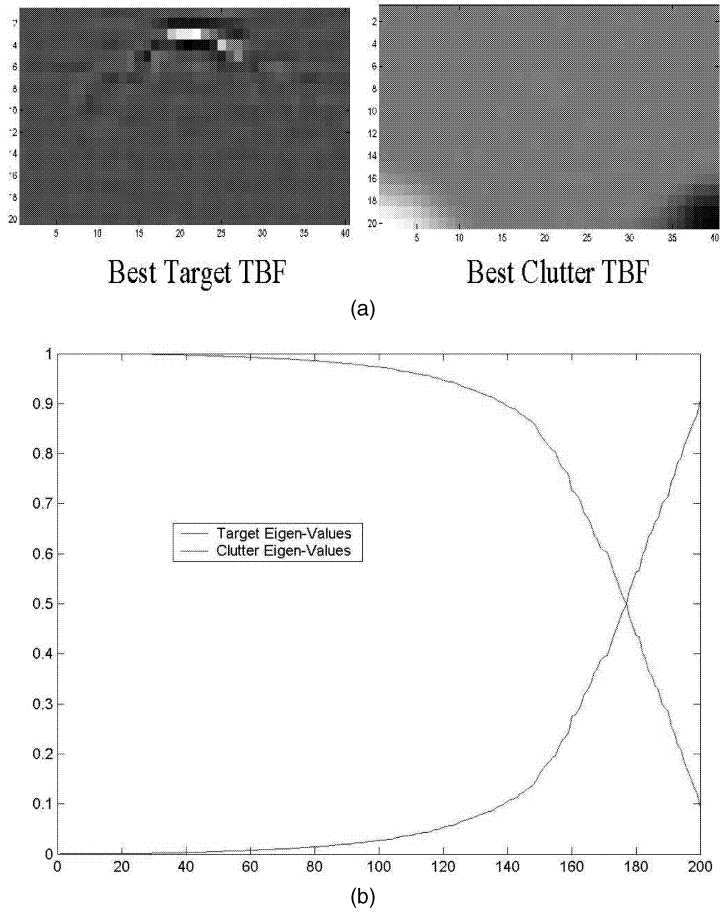

Fig. 5. Best target and clutter basis functions are shown above plot of eigenvalues of the two classes. Horizontal axis represents eigenvector number.

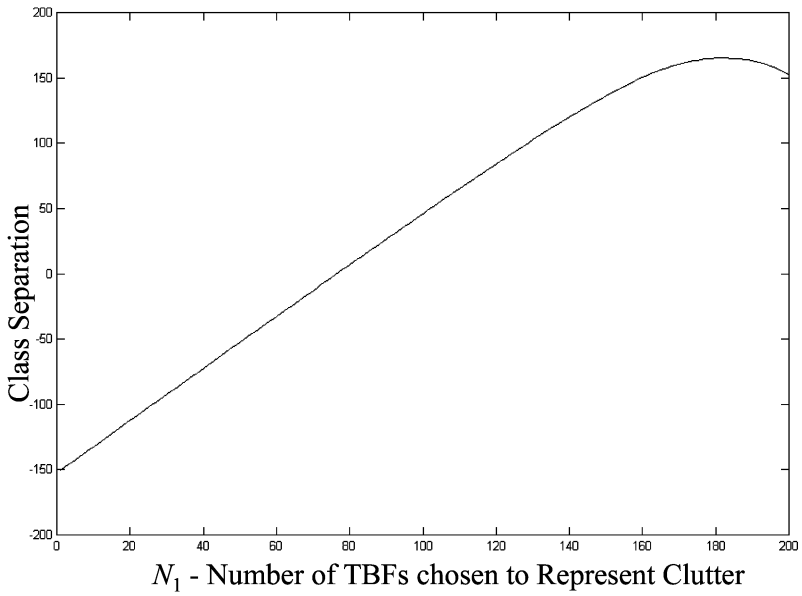

Fig. 6. Separation metric $E_1\{\varphi\} - E_2\{\varphi\}$ is maximum when TBFs to left of eigenvalue cross-over are chosen as $g_i(m,n)$ in (37) while those to right of cross-over are chosen as $f_i(m,n)$.

We tested a variation of the architecture in Fig. 1 that economizes on the throughput requirement of the quadratic filter by correlating the input image only with the target basis functions. The idea is to use the target TBFs $f_i(m,n)$ to detect potential targets and then project the local regions onto the clutter TBFs $g_i(m,n)$ to reduce the number of full correlation operations. The result of processing the scene in Fig. 3 with the

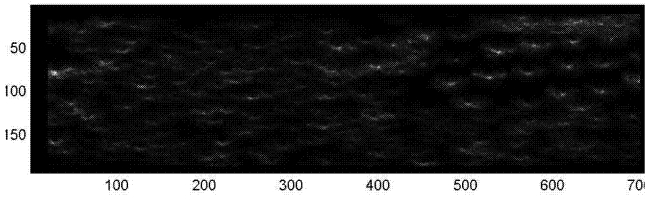

Fig. 7. Target detection map obtained by filtering input image using top 11 target basis functions and squaring and adding results. Energy concentration (peaks) in image indicate position of potential targets.

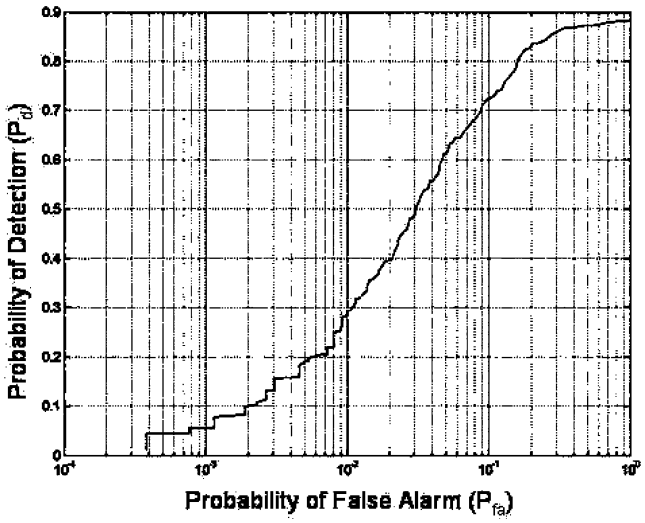

Fig. 8. Detection ROC curve using TBFs.

18 target TBFs (and squaring and adding the outputs) is shown in Fig. 7. The peaks (energy concentration) indicate the presence of potential targets. The position of the peaks is a good indication of the locations of the targets. A 20×40 region of the input image centered at the location of each peak was projected on the clutter TBFs. The final detection metric was the difference between the value of the peak (the estimate of target energy) and the projected clutter energy. Per the design of the quadratic filter, we expect this measure to be large for targets and small for clutter.

The results of processing the frames over all available passes at the targets are shown in Fig. 8. The receiver operating characteristic (ROC) curve shows that on this data, 80% of the targets can be detected with a false alarm rate of approximately 10%. This performance is comparable to other results reported on this data set using linear MACE filters. The advantage is however that 1) far fewer filters filtering operations are required, and 2) the filter outputs are combined into a single detection map so that the problem of selecting among individual filter outputs is avoided.

V. CONCLUSION

In this paper, we introduced a method for designing and implementing QCFs for shift-invariant target detection in imagery. The QCFs are a quadratic classifier that operates directly on the image data without feature extraction or segmentation. In this sense, the QCFs retain the main advantages of linear correlation filters while offering significant improvements in other respects. In addition to better performance, the QCFs produce a single output surface that is easier to process than multiple individual surfaces produced by a bank of separately trained linear filters. Not only is more processing required to detect peaks in the outputs of multiple filters, but choosing a winner among them is an error prone task. On the other hand, all channels in a QCF work together to optimize the same performance metric and produce a combined output that leads to considerable simplification of the postprocessing scheme. The key items covered in the paper follow.

1) Formulation quadratic discriminant correlation filters for target detection in images.
2) Two different methods for designing basis functions (referred to as TBFs) that optimize the QCF performance criterion.
3) An efficient architecture for implementing QCFs.
4) A case study of the proposed approach for detecting targets in LADAR imagery.

Future work will be directed towards new and more powerful methods for designing TBFs (including frequency domain and multiresolution techniques), and further generalizations of the QCF that leads to

performance improvements. We will also investigate noise properties, detection variance, and distortion tolerance of the QCFs, and assess their performance for multiclass target recognition applications.

REFERENCES

[1] Starch, J., Sharma, R., and Shaw, S. (1997)
A unified approach to feature extraction for model based ATR.
In *Proceedings of SPIE, Algorithms for SAR Imagery III, Vol. 2757*, 1997, 294–305.

[2] Casasent, D., and Shenoy, R. (1997)
Feature space trajectory for distorted object classification and pose estimation in SAR.
Optical Engineering, **36** (1997), 2719–2728.

[3] Bhanu, B., and Ahn, J. (1998)
A system for model-based recognition of articulated objects.
In *Proceedings of the International Conference on Pattern Recognition*, 1998, 1812–1815.

[4] Der, S. Z., Zheng, Q., Chellappa, R., Redman, B., and Mahmoud, H. (2002)
View based recognition of military vehicles in LADAR imagery using CAD model matching.
In B. Javidi (Ed.), *Image Recognition and Classification, Algorithms, Systems and Applications*.
New York: Marcel Dekker, Inc., 2002, 151–187.

[5] Chan, L. A., Der, S. Z., and Nasrabadi, N. M. (2002)
Neural based target detectors for multi-band infrared imagery.
In B. Javidi (Ed.), *Image Recognition and Classification, Algorithms, Systems and Applications*, New York: Marcel Dekker, Inc., 2002, 1–36.

[6] Torreiri, D. (1996)
A linear transform that simplifies and improves neural network classifiers.
In *Proceedings of International Conference on Neural Networks, Vol. 3*, 1996, 1738–1743.

[7] Vijaya Kumar, B. V. K. (1992)
Tutorial survey of composite filter designs for optical correlators.
Applied Optics, **31** (1992), 4773–4801.

[8] Mahalanobis, A., Vijaya Kumar, B. V. K., Sims, S. R. F., and Epperson, J. (1994)
Unconstrained correlation filters.
Applied Optics, **33** (1994), 3751–3759.

[9] VanderLugt, A. (1964)
Signal detection by complex spatial spatial filtering.
IEEE Transactions on Information Theory, **IT-10** (1964), 139–145.

[10] Duda, R. O., and Hart, P. E. (1973)
Pattern Classification and Scene Analysis.
New York: Wiley, 1973.

[11] Fukunaga, K., and Koontz, W. L. G. (1970)
Representation of random processes using the finite Karhunen-Loève expansion.
IEEE Transactions on Information and Control, **16**, 1 (1970), 85–10.

[12] Leger, J. R., and Lee, S. H. (1979)
Coherent optical implementation of generalized two-dimensional transforms.
Optical Engineering, **18** (1979), 518–523.

[13] Leger, J. R., and Lee, S. H. (1982)
Image classification by an optical implementation of the Fukunaga-Koontz transform.
Journal of the Optical Society of America, **72** (1982), 556–564.

[14] Mahalanobis, A., Vijaya Kumar, B. V. K., and Sims, S. R. F. (1996)
Distance classifier correlation filters for multi-class target recognition.
Applied Optics, **35** (1996), 3127–3133.

[15] Mahalanobis, A., and Vijaya Kumar, B. V. K. (1997)
Polynomial filters for higher order correlation and multi-input information fusion.
In *Euro American Workshop on Optoelectronic Information Processing*, SPIE Optical Engineering Press, Barcelona, Spain, June 1997, 221–231.

[16] Mahalanobis, A., Ortiz, L., and Vijaya Kumar, B. V. K. (1999)
Performance of the MACH/DCCF algorithms on the 10-class public release MSTAR data set.
Proceedings of SPIE, Algorithms for Synthetic Aperture Radar Imagery VI, Vol. 3721, Apr. 1999, 285–291.

[17] Mahalanobis, A., and Singh, H. (1993)
Application of correlation filters for texture recognition.
Applied Optics, **33**, 11 (Apr. 1993), 2173–2177.

[18] Loève, M. M. (1955)
Probability Theory.
Princeton, NJ: VanNostrand, 1955.

Abhijit Mahalanobis completed his B.S. degree with Honors at the University of California, Santa Barbara in 1984. He then joined the Carnegie Mellon University, Pittsburgh, PA, and received the M.S. and Ph.D. degrees in 1985 and 1987, respectively.

Prior to joining Lockheed Martin, Mr. Abhijit worked at Raytheon (formerly Hughes) in Tucson, and was a faculty member at the University of Arizona. He is now principle research engineer at Lockheed Martin–Orlando, and is currently the technical lead for ATR programs in the Research and Technology group. His main interest are in multisensor automatic target recognition, pattern recognition, and image processing. He has over 100 journal and conference publications in this area. He has pioneered new approaches in the field of correlation pattern recognition which are being pursued by many research groups in the U.S. and abroad.

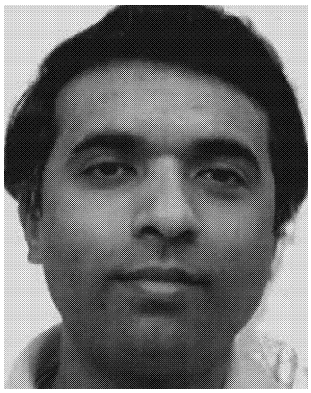

Dr. Abhijit is currently an associate editor for *Applied Optics*. He is a frequent reviewer of papers for OSA and IEEE journals, and serves on the organizing committee for the SPIE conferences. He is also currently serving on the Science and Engineering Council for OSA. He also holds two patents, contributed several book chapters, and edited special issues of several journals including *Optical Engineering*, *Applied Optics* and the *Pattern Recognition*. He received the Hughes Business unit Patent Award in 1998 and was elected as a member of the Raytheon Honors program in 1999 for technical contributions and leadership. He was elected a fellow of the Society of Photo Instrumentation Engineers (SPIE) in 1997 for his work on automatic target recognition. He was also recognized as the Innovator of the Year by the State of Arizona in 1999. Recently, he was elected as a distinguished member of the technical staff at Lockheed Martin. He is also a recipient of the company's Excellence Award in 2002.

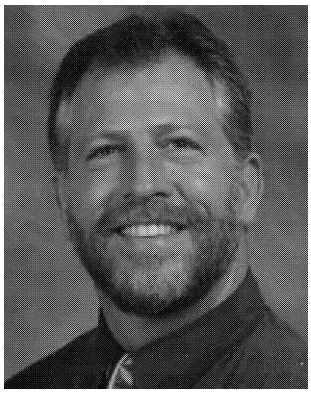

Robert Muise arned his B.S. degree in pure mathematics in 1988 and earned his M.S. and Ph.D. degrees in applied mathematics in 1990 and 2003, respectively, all from the University of Central Florida, Orlando.

He is a senior staff research engineer at Lockheed Martin–Orlando. He is a member of their Research & Technology Automatic Target Recognition and Image Processing Team. His research interests are in image and signal processing for pattern recognition, automatic target detection, and recognition applications. In addition to his work at Lockheed Martin, Robert is part of the faculty in the Department of Mathematics at the University of Central Florida.

S. Robert Stanfill holds dual B.S. degrees in physics and electrical engineering from the University of Florida, Gainesville, dual M.S. degrees in physics and electrical engineering from the Ohio State University, Columbus, and a Ph.D. in electrical engineering from the University of Florida, Gainesville.

He is a senior staff research engineer at Lockheed Martin–Orlando and is a member of their Research & Technology Automatic Target Recognition and Image Processing Team.

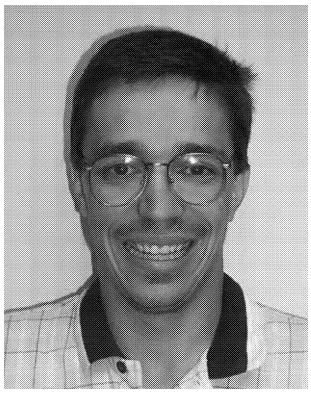

Alan Van Nevel received the B.S. degree (with honors) from Truman State University, Kirksville, MO, in 1990, and the M.S. and Ph.D. in physics in 1993 and 1996, from the University of Missouri–Columbia.

He is a research physicist at the Naval Air Warfare Center, Weapons Division in China Lake, CA, and is currently the head of the Image and Signal Processing Branch in the Research Department. His current interests are in pattern recognition, image processing, target recognition, and application of physical principles to image processing.

Dr. Van Nevel has chaired several sessions on LADAR ATR for the SPIE ATR conference, in addition to publishing several papers on ATR.